

Analysis of isoprenoid biosynthesis in peroxisomal-deficient Pex2 CHO cell lines

Nahla Aboushadi and Skaidrite K. Krisans¹

Department of Biology, San Diego State University, San Diego, CA 92182

Abstract ZR-78 and ZR-82 cells are two peroxisomal-deficient Chinese hamster ovary (CHO) cell mutants. These cells lack normal peroxisomes and show reduced levels of plasmalogen synthesis and other peroxisomal functions attributed to the deficiency of peroxisomal matrix enzymes. As we have recently identified two HMG-CoA reductase proteins in CHO cells, a 97 kDa reductase localized in the ER and a 90 kDa reductase protein localized in peroxisomes, this enabled us to study the two reductase proteins for the first time in peroxisomal-deficient CHO cells. In this study we report the results of a detailed analysis of the isoprenoid biosynthetic pathway in the peroxisomal-deficient CHO cell lines ZR-78 and ZR-82. We demonstrate that total HMG-CoA reductase activity is significantly reduced in the peroxisomal-deficient cells as compared to the wild type cells. Analysis of the two reductase proteins in permeabilized cells indicated that in the ZR-78 and ZR-82 cells the 90 kDa peroxisomal reductase protein was mainly localized to the cytosol. We further show that the rates of both sterol (cholesterol) and non-sterol (dolichols) biosynthesis were significantly lower in the peroxisomal-deficient cells, when either [³H] acetate or [³H] mevalonate was used as substrate. In contrast, the rate of dolichol biosynthesis in the peroxisomal-deficient cells was similar to that of the wild type cells when incubated with [³H] farnesol. In addition, we demonstrate that the peroxisomal-deficient cells exhibited increased rates of lanosterol biosynthesis as compared to wild type cells. The results of this study provide further evidence for the essential requirement of peroxisomes for cholesterol biosynthesis as well as for dolichol production.—Aboushadi, N., and S. K. Krisans. Analysis of isoprenoid biosynthesis in peroxisomal-deficient Pex2 CHO cell lines. *J. Lipid Res.* 1998. 39: 1781–1791.

Supplementary key words peroxisomes • cholesterol • dolichol

Recent studies by our group and others have demonstrated that a number of the enzymes of the isoprenoid biosynthetic pathway are localized to peroxisomes (1). These include acetoacetyl-CoA thiolase (2, 3), 3-hydroxy-3-methylglutaryl coenzyme A (HMG-CoA) synthase (4), HMG-CoA reductase (5–7), mevalonate kinase (8, 9), phosphomevalonate kinase (10), phosphomevalonate decarboxylase (10), isopentenyl diphosphate (IPP) isomerase

(11), and farnesyl diphosphate (FPP) synthase (12). Mevalonate kinase, IPP isomerase, and FPP synthase were shown to be localized predominantly to peroxisomes, suggesting that the conversion of mevalonate to FPP may occur exclusively in peroxisomes (8, 9, 11, 12). This is further supported by the observation that mevalonate kinase (13), phosphomevalonate kinase (14), mevalonate diphosphate decarboxylase (15), and IPP isomerase (11, 16) all contain a putative peroxisomal targeting signal (PTS1 or PTS2) (17). In a recent study we provided direct evidence that the putative PTS1 of IPP isomerase is necessary for peroxisomal targeting (11). In addition, four of the enzyme activities (dihydrolanosterol oxidase, steroid-14-reductase, steroid-3-ketoreductase, and steroid-8-isomerase) involved in the conversion of lanosterol to cholesterol have been reported to be present in peroxisomes (18).

The indispensable role of the peroxisomal enzymes in isoprenoid biosynthesis is also evident in humans afflicted with the recessive inherited peroxisomal disorders (PDs), for example, Zellweger syndrome (ZS), where normal peroxisomes are absent from the cells of these patients (19, 20). The lack of normal peroxisomes in these cells results in both the cytosolic localization and reduced levels of the peroxisomal matrix enzymes. The consequence of this is reflected in the absence or reduced activity of independent peroxisomal enzymatic pathways such as plasmalogen biosynthesis, degradation of very long chain fatty acids, accumulation in bile acid intermediates, and low plasma cholesterol levels (19, 20). Lower rates of cholesterol biosynthesis are also apparent in skin fibroblasts derived from these patients (21, 22).

A number peroxisomal-deficient Chinese hamster ovarian (CHO) cell line mutants have been isolated. Two such cell lines are the ZR-78 and the ZR-82 mutants (23). Similar to the ZS fibroblasts, the peroxisomal-deficient CHO cell lines, ZR-78 and ZR-82 lack normal peroxisomes and

Abbreviations: CHO, Chinese hamster ovary; HMG-CoA, 3-hydroxy-3-methylglutaryl coenzyme A; LPDS, lipoprotein-deficient serum; BSA, bovine serum albumin; TLC, thin-layer chromatography; ER, endoplasmic reticulum; IPP, isopentenyl diphosphate; FPP, farnesyl diphosphate.

¹To whom correspondence should be addressed.

show reduced levels of plasmalogen synthesis and other peroxisomal functions attributed to the deficiency of peroxisomal matrix enzymes (24, 25). Thus, these cells would also be expected to exhibit lower rates of cholesterol biosynthesis similar to that reported in ZS fibroblasts (21, 22). Surprisingly however, a recent study reported both higher activity levels of HMG-CoA reductase, the rate-limiting enzyme in isoprenoid biosynthesis, and higher rates of cholesterol biosynthesis in the peroxisomal-deficient cells as compared to the wild type CHO cells (26). These results prompted us to investigate these cell lines in order to discern how peroxisomal-deficient cells, which should be deficient in enzymes required for cholesterol synthesis, can display higher rates of cholesterol biosynthesis. Furthermore, as we have recently identified two HMG-CoA reductase proteins in CHO cells, a 97 kDa reductase localized in the ER and a 90 kDa reductase protein localized in peroxisomes (7), this enabled us by use of cell permeabilization techniques to determine the subcellular localization of the 90 kDa reductase protein in the peroxisomal-deficient cells.

In this study we report the results of a detailed analysis of the isoprenoid biosynthetic pathway in the peroxisomal-deficient CHO cell lines, ZR-78 and ZR-82.

EXPERIMENTAL PROCEDURES

Materials

Biochemicals were purchased from Sigma. Electrophoresis supplies, AG1-X8-200-400 mesh formate resin and Trans-Blot Transfer Medium (used for Western analysis) were purchased from Bio-Rad. All cell culture media and fetal calf serum were purchased from Life Technologies, Inc. Lipoprotein-deficient media was obtained from PerImmune. dl-3-[glutaryl-3-¹⁴C]3-hydroxy-3-methylglutaryl coenzyme A, [26-¹⁴C]cholesterol, [³H]acetic acid, sodium salt and RS-[5-³H(N)]mevalonolactone were purchased from DuPont NEN. [1-³H]farnesol was purchased from American Radiolabeled Chemicals Inc. and ³H-labeled dihydrolanosterol was a generous gift from Dr. Charles Baum.

Cell culture

CHO cells were maintained in 1:1 Dulbecco's modified Eagle's media: F12, supplemented with 5% fetal calf serum (FCS), fungizone and pen/strep, in a 37°C incubator with 5% CO₂ atmosphere. ZR-78 and ZR-82 cells were maintained in 1:1 Ham's: F12 media and supplemented with 10% (FCS). Twenty-four h prior to all experiments, mutant and wild type cells were transferred to media supplemented with 5% lipoprotein-deficient serum (LPDS). The ZR-78 and 82 cells were a generous gift from Dr. Raphael A. Zoeller.

Cell permeabilization

Care was taken to seed an equal number of CHO, ZR-78 and ZR-82 cells at a density of 4.0×10^4 cells/60-mm plate and grown to 60% confluence. Cells were transferred to media supplemented with 5% LPDS 24 h prior to the experiment. The day of the experiment, the media was aspirated off the plates and the plates were washed twice with ice-cold KH buffer (50 mM HEPES, 110 mM KOAc, pH 7.2). The plates were then transferred to ice and the cells were incubated while shaking for 5 min in KHM buffer containing 20 µg/ml digitonin, 20 mM HEPES, 110 mM

KOAc, and 2 mM MgOAc, pH 7.2. The digitonin solution was aspirated off the cells and the cells were washed twice with ice-cold KH buffer and subsequently allowed to incubate in KH buffer for 30 min (10, 27). This procedure allows the cells to remain attached to the plates. Cells were scraped into 50 mM KPO₄, pH 7.0, containing 200 mM NaCl, 30 mM EDTA, 10 mM DTT (KEND) and used for enzyme activities determinations. Control cells were treated similarly, washed with the same buffer lacking digitonin, scraped in KEND buffer, and centrifuged at 12,000 RPM. Pellets were resuspended in KEND plus 0.2% triton and homogenized by hand with 20 strokes with an Eppendorf glass pestle before performing enzyme assays on the samples.

Marker enzyme assays

The activities of phosphoglucose isomerase, esterase, and catalase were measured as described (10). Protein concentration was determined by the BCA method (Pierce) using bovine serum albumin (BSA) as a standard.

HMG-CoA reductase assay

Only freshly prepared cell extracts were assayed. The samples were preincubated for 30 min at 37°C before the addition of substrate to insure the inactivation of HMG-CoA lyase activity. The preincubation mixture consisted of 150 µl of KEND buffer, pH 7.0, containing 100 µg of whole cell extract protein. After preincubation, the reaction mixture (150 µl) containing 208 µM [¹⁴C]HMG-CoA and 2 mM NADPH (final concentration) and 20,000 dpm of [³H]-mevalonate in KEND buffer was added. The samples were incubated at 37°C for 40 min and the reaction was stopped by the addition of 30 µl of 10.5 N HCl. Control samples containing BSA or lacking NADPH were routinely included. After centrifugation, HMG-CoA was separated from the product (mevalonolactone) by AG1-X-8 formate resin ion exchange columns as described (7).

SDS gel electrophoresis and immunoblotting techniques

We have recently shown that separation of the 97 kDa endoplasmic reticulum (ER) reductase from the 90 kDa peroxisomal reductase is dependent upon the length of the gel and percent of acrylamide (7), therefore 12.5 cm gels consisting of 7.5% acrylamide were used. Polyclonal antibodies made to the ER HMG-CoA reductase were a generous gift from Dr. Peter Edwards (28). Western blots for thiolase and PMP 26 were performed as previously described (8). The anti-thiolase and anti-PMP 26 antibodies were a generous gift from Dr. Suresh Subramani.

Determination of rate of biosynthesis of cholesterol, lanosterol, and dolichols

Cells were grown to 60% confluence on 100-mm plates in standard media, and transferred to media containing 5% LPDS 24 h prior to incubating with one of the following substrates: 5 µCi of [³H] acetate, 50 µM (1.1×10^5 dpm/nmol) for 12 h; or 50 µCi of [³H] mevalonate, 5 mM (1.1×10^4 dpm/nmol) for 4 h; or 50 µCi of [³H]farnesol, 50 µM (1.1×10^6 dpm/nmol) for 12 h and 24 h; or 6 µCi of [³H]dihydrolanosterol, 6.2 µM (1.00×10^6 dpm/nmol) for 24 h. After incubation, the media was aspirated off the plates and the plates were rinsed three times with cold PBS buffer, pH 7.0, and scraped in KH buffer pH 7.2. Cell extracts were centrifuged at 12,000 rpm. Pellets were resuspended in KH buffer plus 1% triton and homogenized by hand with 20 strokes with a glass pestle. A sample of whole cell extract was taken for protein determination and rate of cholesterol and dolichols biosynthesis was determined as described (29) with several modifications. Cell ex-

tracts were saponified with 1 ml 60% KOH at 70°C for 1 h, and after addition of ¹⁴C-radiolabeled cholesterol for use as an internal standard, samples were extracted with diethyl ether, treated with an equal volume of 5% acetic acid, and the ether layer was taken to dryness at 40°C under a stream of nitrogen. The residue was dissolved in 2 ml CH₃OH and 0.2 ml of water was added. The sample was then transferred to a C18 column equilibrated with CH₃OH–H₂O 10:1. After application of the sample, the column was treated with 7 ml CH₃OH–H₂O 10:1 to first elute the fatty acid fraction. Then 5 ml of CH₃OH was added to elute the sterol fraction and finally 4 ml hexane–2-propanol–methanol 1:1:6 was added to elute the dolichol–phosphate fraction. For the analysis of sterols, the CH₃OH fraction was dried under nitrogen, redissolved in 500 μl of chloroform, and separated by thin-layer chromatography (TLC) (hexane–diethyl ether 50:50). Cholesterol is well resolved from lanosterol and squalene in this TLC system.

RESULTS

The ZR-78 and ZR-82 cell lines are two well-characterized peroxisome-deficient CHO cell mutants (24, 25). Because peroxisomal β-oxidation enzymes are severely deficient in these cell lines, we tested these cells for the levels of peroxisomal β-oxidation thiolase, a peroxisomal matrix enzyme. As demonstrated in Fig. 1, thiolase levels were significantly reduced in the cell extracts from peroxisomal-deficient cells as compared to CHO cells, verifying that these cells are deficient in the peroxisomal matrix enzyme thiolase.

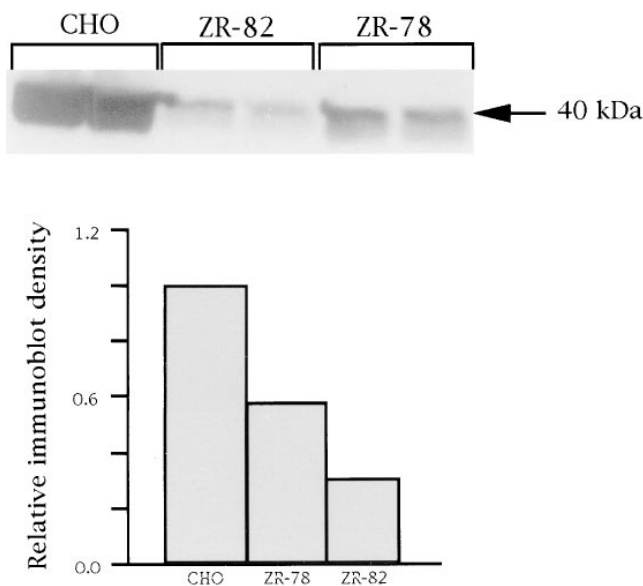


Fig. 1. Immunoblotting analysis of thiolase in whole cell extracts from CHO, ZR-78, and ZR-82 cells. CHO and peroxisomal-deficient ZR-78 and ZR-82 cells were cultured by standard methods. The cells were harvested at 70–80% confluency. Duplicate samples (200 μg) from each cell line were electrophoresed and immunoblotted using anti-thiolase IgG. Blots were then incubated with protein A-horse radish peroxidase and detected with Amersham's enhanced chemiluminescence reagent. The immunoblot was scanned on a Molecular Dynamics Densitometer and quantitated by use of ImageQuant.

Determination of HMG-CoA reductase activity in CHO, ZR-78, and ZR-82 cell extracts

The primary site at which cells regulate the rate of isoprenoid biosynthesis is at the rate-limiting step of sterol biosynthesis, the conversion of HMG-CoA to mevalonate by HMG-CoA reductase (30). HMG-CoA reductase has been localized to both the endoplasmic reticulum and peroxisomes (5–7). The ER HMG-CoA reductase is a transmembrane glycoprotein of 97 kDa and its regulation is well characterized (30). We have recently demonstrated that the peroxisomal form of HMG-CoA reductase is 90 kDa (7). Very little information is available regarding the function and regulation of the peroxisomal reductase (1). To address whether the absence of normal peroxisomes alters the total reductase activity levels in the peroxisomal-deficient cells, we measured total reductase activities in the three cell lines. Total reductase activity measurements showed that the mean HMG-CoA reductase activities in the ZR-78 and ZR-82 cells were 130 pmol/min per mg and 82 pmol/min per mg, respectively (Fig. 2). Whereas, the reductase activity in CHO cells was 240 pmol/min/mg (Fig. 2). Thus, total reductase activity in the peroxisomal-deficient cells is significantly lower than in CHO cells.

We have previously observed by immunoelectron microscopy that the labeling of the peroxisomal reductase was localized to the matrix of the organelle (5, 6). In order to determine the localization of the 90 kDa peroxisomal reductase in the peroxisomal-deficient cells and in the CHO cells, we utilized a selective cell permeabilization technique (10). This technique is based on the use of digitonin, which permeabilizes cells by complexing with cholesterol. As the membranes of most cell organelles are devoid of cholesterol, low concentrations of digitonin will complex principally with the plasma membrane. This results in the loss of the cytosolic fraction, while maintaining the integrity of the intracellular organelles.

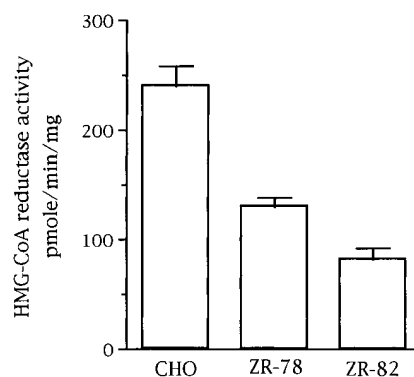


Fig. 2. HMG-CoA reductase activity measurements and immunoblotting of whole cell extracts from CHO, ZR-78, and ZR-82 cells. CHO and peroxisomal-deficient ZR-78 and ZR-82 cells were cultured by standard methods. The cells were harvested at 70–80% confluency and homogenized in the presence of Triton X-100. One hundred μg of cell extract from each cell line was assayed for HMG-CoA reductase activity. Each value represents the average of nine experiments, performed in duplicate, ±SE. For ZR-78 and ZR-82, $P < 0.0001$ versus control cells).

Verification of the selective permeabilization of the plasma membrane and subsequent release of the cytosolic components

The selectivity of the cell permeabilization technique was confirmed by measuring the marker enzymes of the various organelles in permeabilized and control cells. We determined the activities of esterase (a marker enzyme for the ER), catalase (the marker enzyme for peroxisomes), and phosphoglucose isomerase (PGI) (a marker enzyme for the cytosolic fraction). **Table 1** illustrates the results. In CHO cells, there was no change in total activity for esterase or catalase, whereas PGI, as expected, was measurable only in intact cells but not in the permeabilized cells. The protein concentration in permeabilized cells was approximately 30–50% less than that of intact cells as a result of the loss of the cytosolic protein content. In the peroxisomal-deficient cells, similar activities of esterase were measured in the control and permeabilized cells. However, in the peroxisomal-deficient cells, PGI and catalase activities were significantly reduced in the permeabilized cells, verifying a cytosolic localization of catalase in the mutant cells. In previous studies utilizing the same technique, we have demonstrated by immunofluorescence labeling that the organelles of the cell remain intact after permeabilization while the cytosolic contents disappear (10).

Measurement of HMG-CoA reductase activity in control and permeabilized cells

We also determined HMG-CoA reductase activities in the peroxisomal-deficient cells and CHO cells before and after cell permeabilization. The CHO cells showed no difference in total reductase activity before or after digitonin treatment (Table 1), whereas, the mutant cells' reductase activity was reduced in the permeabilized cells, suggesting that at least a portion of the reductase activity had a cytosolic localization.

Immunoblotting of CHO, ZR-78, and ZR-82 cell extracts for HMG-CoA reductase after cell permeabilization

Cell extracts of permeabilized and intact CHO and peroxisomal-deficient cells were immunoblotted for HMG-CoA reductase. In CHO cells, both the 97 kDa and the 90 kDa reductase proteins were detectable in the permeabi-

lized and the intact cell extracts (**Fig. 3**, panel A). In the ZR-78 and ZR-82 cells, the 97 kDa protein was present in both permeabilized and intact cell extracts; however, the 90 kDa protein was mainly detected in intact cell extracts (**Fig. 3**, panel A). In the ZR-78 and ZR-82 permeabilized cell extracts, the 90 kDa protein was either undetectable (ZR-82) or significantly decreased (ZR-78). These data suggest that in the peroxisomal-deficient cell lines the 90 kDa peroxisomal reductase is predominantly localized in the cytosol similar to that demonstrated for other peroxisomal matrix enzymes. We confirmed that the digitonin treatment did not affect the integrity of peroxisomal membranes by immunoblotting the cell extracts of permeabilized and intact cells using an antibody against a 26 kDa peroxisomal integral membrane protein (PMP 26). As PMP 26 is a membrane protein, it would be expected to be present in the "peroxisomal membrane ghosts" detected in peroxisomal-deficient cells. PMP 26 was present in all three cell lines before and after digitonin treatment (**Fig. 3**, panel B), verifying that digitonin treatment did not affect the integrity of peroxisomal membranes.

The isoprenoid pathway requires the participation of enzymes located in several cellular compartments. **Figure 4** illustrates our current concept of the compartmentalization of cholesterol biosynthesis enzymes (1). The peroxisome contains enzymes for the conversion of acetyl-CoA to FPP. The conversion of acetyl-CoA to HMG-CoA also occurs in the cytosol, with the further conversion of HMG-CoA to mevalonate taking place in the ER and peroxisomes; the conversion of mevalonate to FPP occurs predominately if not exclusively in the peroxisome. The incorporation of FPP into squalene occurs only in the ER, and lastly the metabolism of lanosterol to cholesterol takes place in the ER and may occur also in the peroxisomal compartment. There is some evidence that the incorporation of FPP into dolichols also takes place in the peroxisome (31).

Rate of biosynthesis of cholesterol and dolichols as measured by the incorporation of [³H] acetate

To address the physiological importance of the peroxisomal enzymes in isoprenoid biosynthesis, and to evaluate the effects of the decrease in total reductase activity in the

TABLE 1. Protein, catalase, esterase, PGI, and HMG-CoA reductase activities in control and permeabilized cells

Cells	Protein <i>mg/plate</i>	Catalase	Esterase <i>milliunits/plate</i>	PGI	HMG-CoA <i>nmol/plate</i>
CHO cells					
Control	1.16 ± 0.55	26 ± 1.75	103 ± 4.9	440 ± 10.9	6.21
Permeabilized	0.75 ± 0.04	29 ± 0.91	101 ± 4.2	0	6.97
ZR-78 cells					
Control	0.98 ± 0.19	16 ± 1.44 ^a	107 ± 7.4	399 ± 12.4	4.48
Permeabilized	0.63 ± 0.08	3 ± 1.30 ^a	104 ± 3.1	0	2.1
ZR-82 cells					
Control	1.23 ± 0.14	14 ± 2.50 ^a	110 ± 7.1	413 ± 11.8	2.4
Permeabilized	0.82 ± 0.09	5 ± 1.75 ^a	106 ± 6.4	0	1.3

Values for protein determination and marker enzyme activities represent mean ± SEM. Values for HMG-CoA reductase are the average of two experiments performed in duplicate.

^a*P* < 0.001 of three separate experiments performed in duplicate.

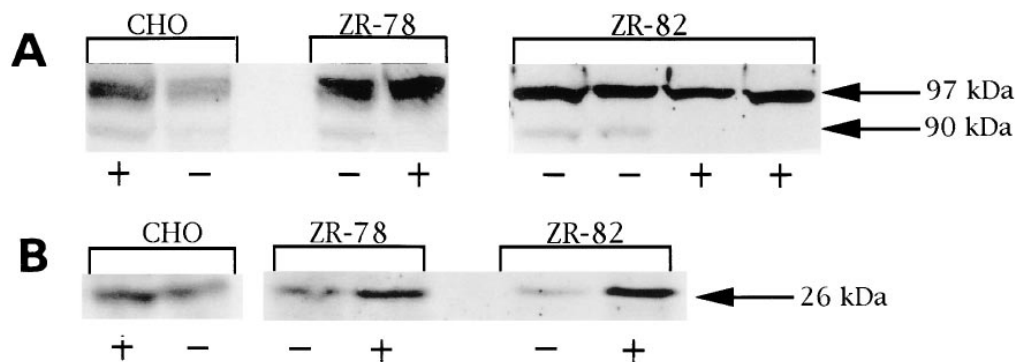


Fig. 3. Immunoblotting analysis of HMG-CoA reductase and PMP-26 in whole cell extracts from CHO, ZR-78, and ZR-82 cells before and after permeabilization of cells by digitonin. CHO and peroxisomal-deficient ZR-78 and ZR-82 cells were permeabilized by digitonin as described in Materials and Methods. Two hundred μg of CHO cells and 300 μg of ZR-78 and ZR-82 before (-), and after digitonin treatment (+), were solubilized, electrophoresed, and immunoblotted using polyclonal anti-reductase IgG (panel A) or anti-PMP-26 IgG (panel B). Blots were incubated with protein A-horseradish peroxidase and detected with Amersham's enhanced chemiluminescence reagent.

peroxisomal-deficient cell lines, we measured the rate of sterols (cholesterol) and non-sterols (dolichols) biosynthesis in the three cell lines after incubating the cells with [^3H] acetate for 12 h. The rates of biosynthesis of cholesterol and dolichols were significantly reduced in the two peroxisomal-deficient cells as compared to the CHO cells (Fig. 5, panels A and B). Cholesterol biosynthesis was inhibited by 63–71% and dolichol biosynthesis was inhibited by 77–78%.

Rate of biosynthesis of cholesterol and dolichols as measured by the incorporation of [^3H] mevalonic acid

To analyze whether the decrease in cholesterol and dolichol biosynthesis observed when using acetate as substrate was solely due to the deficiency in HMG-CoA reductase activity in the peroxisomal-deficient cells or whether the peroxisomal enzymes responsible for the conversion of mevalonate to FPP were also affected in the mutant cell lines, we incubated the peroxisomal-deficient cells and the wild type CHO cells with [^3H]mevalonate for 4 h and determined the rate of cholesterol and dolichols biosynthesis. Similar to that observed for acetate, when mevalonate is used as substrate, the mutant cells again displayed significantly reduced rates of cholesterol and dolichol biosynthesis as compared to the wild type cells (Fig. 6, panels A and B). Cholesterol biosynthesis was inhibited by 78–80% and dolichol biosynthesis was inhibited by 63–75%. The experiments starting with mevalonate were also repeated in the presence of 1 μM lovastatin (a competitive inhibitor of HMG-CoA reductase) to inhibit the production of unlabeled isoprenoid products and thereby avoid the dilution of the radioisotope. There was no significant difference between the percent of inhibition of cholesterol and dolichol biosynthesis in the mutant cells in the presence or absence of lovastatin (data not shown). These results combined with the acetate data suggest that the reduced rates of isoprenoid biosynthesis in the mutant cells are not the sole result of the decreased levels of HMG-CoA reductase activity in the mutant cells.

Rate of biosynthesis of cholesterol and dolichols as measured by the incorporation of [^3H]farnesol

FPP is a key intermediate that serves as a substrate for a number of critical branch-point enzymes. FPP can be converted to squalene by squalene synthase, the first committed enzyme for cholesterol biosynthesis. FPP is also the precursor for dolichols, ubiquinone, farnesylated and geranylgeranylated proteins, and the isoprenoid moiety of heme a. We have previously demonstrated that squalene synthase is localized exclusively in the ER (32), therefore, the conversion of FPP to squalene should not be affected in the mutant cells. However, recent studies suggest that peroxisomes like the ER may participate in the conversion of lanosterol to cholesterol as well as in some of the steps required for dolichols biosynthesis (1, 18, 31). We incubated the cells with [^3H]farnesol for 12 h and 24 h to determine whether peroxisomal-deficient cells have a defect in the conversion of FPP to cholesterol and dolichols. Farnesol has been shown to be converted *in vivo* by phosphorylation reactions to FPP and is thereby available for isoprenoid biosynthesis (33). The rate of dolichol biosynthesis in the peroxisomal-deficient cells was similar to that of the wild type CHO cells (Fig. 7, panels B and D), regardless of the time of incubation. However, the rate of cholesterol biosynthesis decreased in the peroxisomal-deficient cells when measured for 12 h but not when determined over a period of 24 h (Fig. 7, panels A and C).

Rate of biosynthesis of cholesterol as measured by the incorporation of [^3H]dihydrolanosterol

As an additional control for the latter steps in cholesterol biosynthesis, we also incubated the three cell lines with [^3H]dihydrolanosterol for 24 h and measured the rate of cholesterol biosynthesis. To prevent any possible dilution of the radioactive dihydrolanosterol, the cells were first incubated with 1 μM lovastatin. There was no difference in the rate of cholesterol biosynthesis in the mutant cells as compared to wild type CHO cells (Fig. 8).

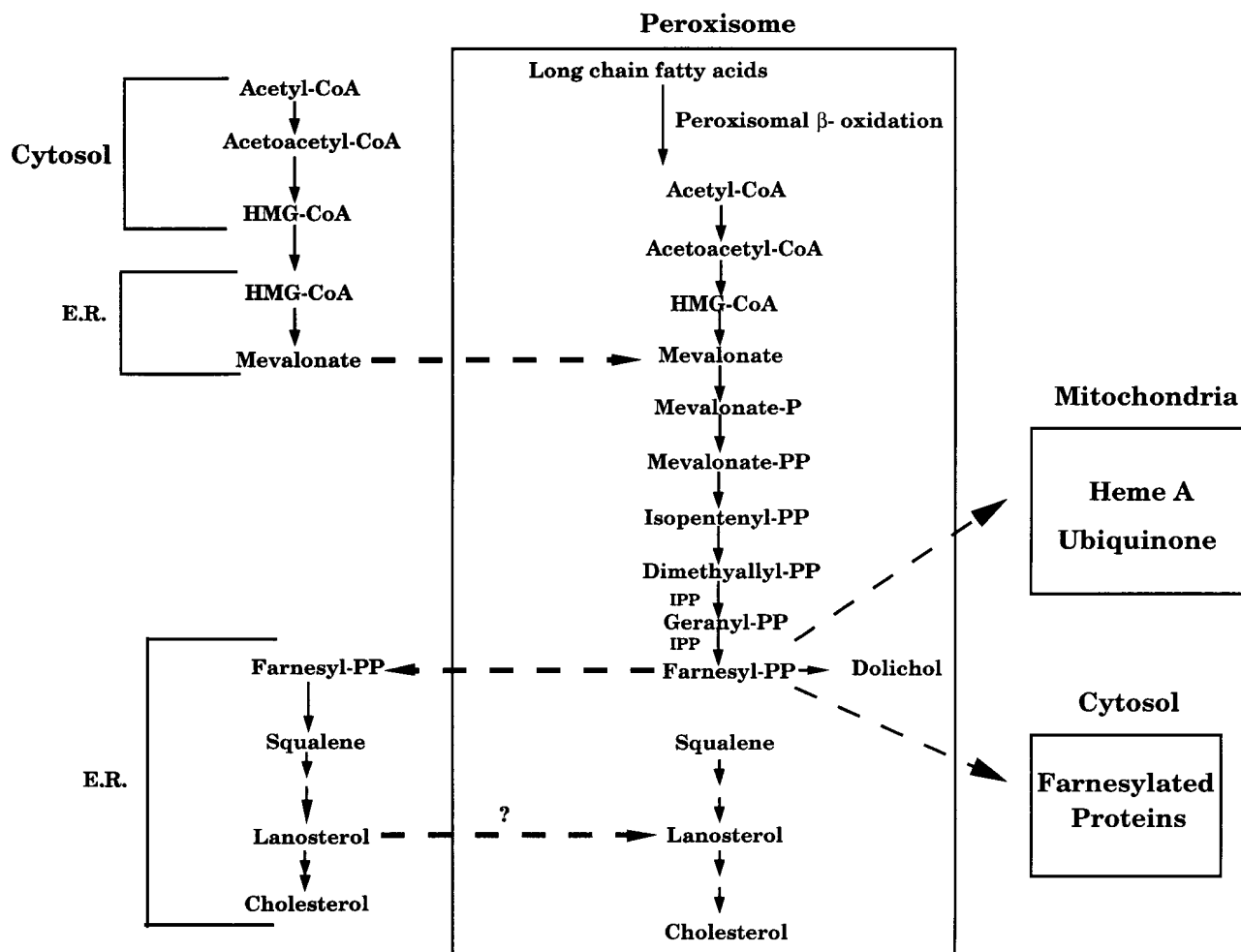


Fig. 4. Compartmentalization of the cholesterol biosynthesis pathway. Peroxisomes contain enzymes for the conversion of acetyl-CoA to FPP. The conversion of acetyl-CoA to HMG-CoA also occurs in the cytosol. The further conversion of HMG-CoA to mevalonate occurs in both the ER and peroxisomes. The metabolism of FPP to squalene occurs exclusively in the ER and lastly, the metabolism of lanosterol to cholesterol occurs in the ER and may also be localized to peroxisomes. FPP is also the precursor for dolichols, ubiquinone, farnesylated and geranylgeranylated proteins, and the isoprenoid moiety of heme a.

Analysis of the rate of lanosterol biosynthesis

In the procedure we utilized to determine cholesterol biosynthesis, we were also able to resolve lanosterol and squalene. Squalene levels were negligible; however, we were able to determine the rate of lanosterol biosynthesis. The mutant cells displayed significantly higher rates of lanosterol biosynthesis, when incubated with mevalonate, farnesol, or dihydrolanosterol, as compared to wild type cells (Fig. 9, panels A, B, and C). The accumulation of lanosterol in the mutant cells was 2- to 2.5-fold higher than that of the CHO cells. These data suggest a role of peroxisomes in the biosynthetic pathway between lanosterol and cholesterol.

DISCUSSION

The ZR-78 and the ZR-82 cells are two CHO cell line mutants that show phenotypic resemblance to the ZS fibroblasts. The mutant cells have peroxisomal membrane

ghosts (peroxisomal structures that contain integral membrane proteins but are devoid of the peroxisomal matrix enzymes), display cytosolic localization of peroxisomal matrix enzymes, and have severe defects in plasmalogen biosynthesis, phytanic acid oxidation, and β -oxidation of very long chain fatty acids (24, 25).

The gene responsible for the mutations in the ZR-78 and ZR-82 cells has been identified to be Pex2p, previously designated as peroxisome assembly factor-1 (PAF-1) (34). The Pex2p gene encodes a peroxisomal integral membrane protein of 35 kDa that is involved in peroxisomal assembly and biogenesis. The mutations in Pex2p in the two cell lines are distinct. The ZR-78 cells have a G to A conversion at nucleotide 737 resulting in a Cys to Tyr alteration at the carboxy terminal of the protein, while the ZR-82 cells contain a nonsense mutation at nucleotide 370 that results in the formation of a premature stop codon (34, 35). A human homologue of Pex2p has been identified and shown to be responsible for the peroxisomal-deficiency defect in one ZS patient (36). In addition, it

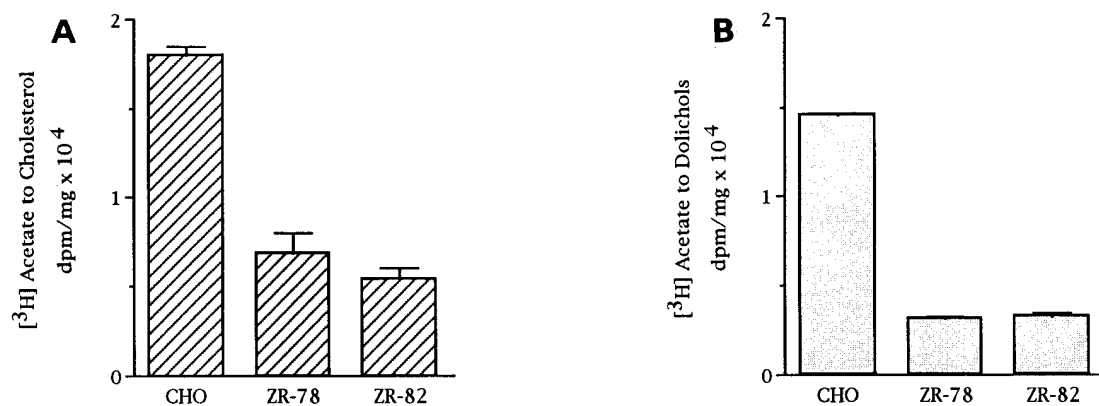


Fig. 5. Rate of biosynthesis of cholesterol and dolichols in CHO and peroxisome-deficient ZR-78 and ZR-82 cells as measured by the incorporation of [³H] acetate. CHO and peroxisomal-deficient ZR-78 and ZR-82 cells were incubated for 12 h with [³H]acetate, 5 μ Ci (1.1×10^5 dpm/nmol/flask) and cholesterol and dolichol biosynthesis was determined as described in Materials and Methods. Panel A, rate of cholesterol biosynthesis expressed as dpm/mg cell protein for CHO, ZR-78 and ZR-82 cells. Each value represents the average of three experiments, performed in duplicate, \pm SE. $P < 0.001$ for ZR-78 and ZR-82 cells vs. control cells). Panel B, rate of dolichol biosynthesis expressed as dpm/mg cell protein for CHO, ZR-78, and ZR-82 cells. Each value represents the average of three experiments, \pm SE. $P < 0.001$ for ZR-78 and ZR-82 cells vs. control cells). The total protein content per flask was between 280 and 400 μ g.

has been recently shown that homozygous Pex2-deficient mice lack normal peroxisomes and display abnormal peroxisomal biochemical parameters, such as increased levels of plasma very long chain fatty acids and a deficiency in plasmalogens (37).

We have recently demonstrated that CHO cells contain two HMG-CoA reductase proteins, the well-characterized 97 kDa protein, localized in the ER and a 90 kDa reductase protein localized in peroxisomes (7).

In the peroxisomal-deficient ZR-78 and ZR-82 permeabilized cells lacking cytosolic components, the 90 kDa reductase protein was significantly reduced or undetectable (Fig. 3, panel A), suggesting a cytosolic localization, consistent with that reported for other peroxisomal matrix

enzymes (38, 39). In addition, as expected, total reductase activity was also reduced in the peroxisomal-deficient permeabilized cells (Table 1). In the control cells, both reductase proteins were visible before and after cell permeabilization (Fig. 3, panel A), and total reductase activity per plate was unchanged as well (Table 1). Given that the reductase activity was reduced in both mutant cell lines, it is likely that part of the decrease in reductase activity was due to the peroxisomal form.

As the reductase antibody is made against the 97 kDa ER form, we have no basis for determining the specificity of this antibody against the 90 kDa peroxisomal form. Previously we demonstrated that in the UT2* cell line expressing only the 90 kDa peroxisomal protein, the reduc-

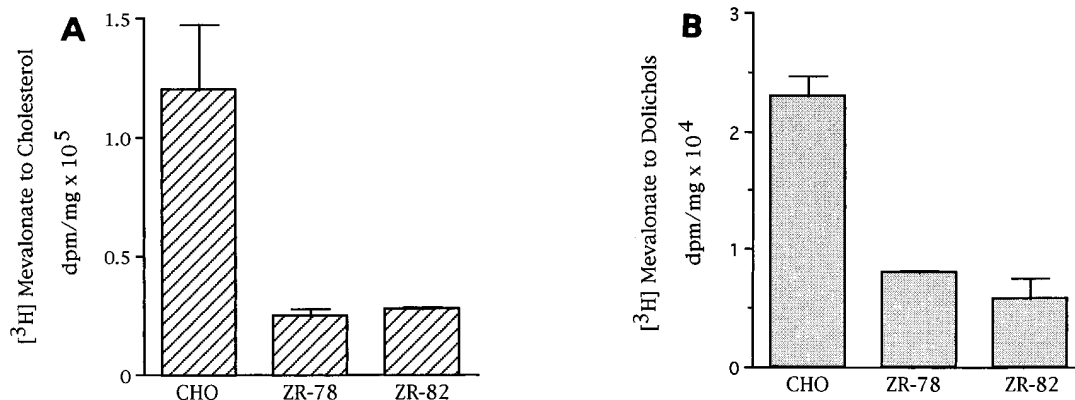


Fig. 6. Rate of biosynthesis of cholesterol and dolichols in CHO and peroxisome-deficient ZR-78 and ZR-82 cells as measured by the incorporation of [³H]mevalonate. CHO and peroxisomal-deficient ZR-78 and ZR-82 cells were incubated for 4 h with [³H]mevalonate, 50 μ Ci (1.1×10^4 dpm/nmol/flask) and cholesterol and dolichol biosynthesis was determined as described in Materials and Methods. Panel A, rate of cholesterol biosynthesis expressed as dpm/mg cell protein for CHO, ZR-78 and ZR-82 cells. Each value represents the average of three experiments, performed in duplicate, \pm SE ($P < 0.001$ for ZR-78 and ZR-82 cells vs. control cells). Panel B, rate of dolichol biosynthesis expressed as dpm/mg cell protein for CHO, ZR-78 and ZR-82 cells. Each value represents the average of three experiments, \pm SE ($P < 0.001$ for ZR-78 and ZR-82 cells vs. control cells). The total protein content per flask was between 200 and 320 μ g.

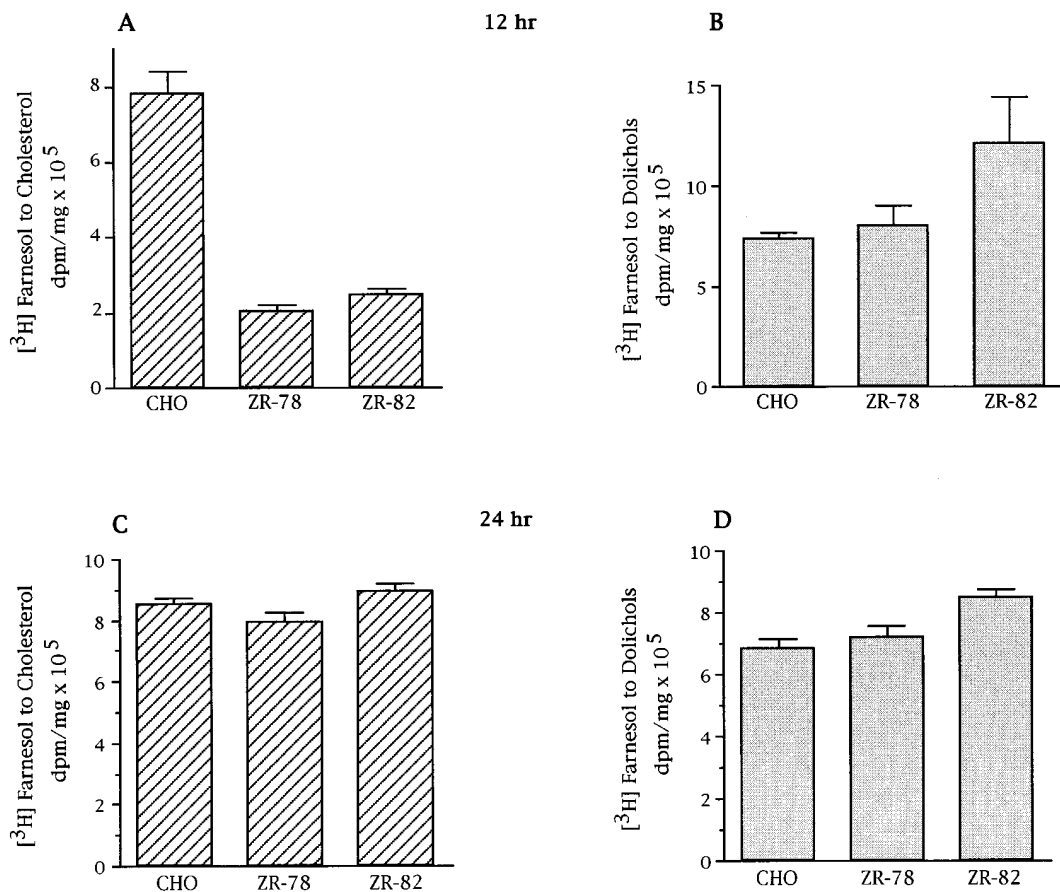


Fig. 7. Rate of biosynthesis of cholesterol and dolichols in CHO and peroxisome-deficient ZR-78 and ZR-82 cells as measured by the incorporation of [³H]farnesol. CHO and peroxisomal-deficient ZR-78 and ZR-82 cells were incubated for 12 and 24 h with [³H]farnesol 5 μ Ci (1.1×10^6 dpm/nmol/per flask) and cholesterol and dolichol biosynthesis was determined as described in Materials and Methods. Panel A, rate of cholesterol biosynthesis after 12 h incubation, expressed as dpm/mg cell protein for CHO, ZR-78 and ZR-82 cells. Each value represents the average of three experiments, \pm SE ($P < 0.01$ for ZR-78 and ZR-82 cells vs. control cells). Panel B, rate of dolichol biosynthesis, after 12 h incubation, expressed as dpm/mg cell protein for CHO, ZR-78 and ZR-82 cells. Each value represents the average of three experiments, \pm SE. There is no significant difference between the ZR-78 and ZR-82 cells and control cells. Panel C, rate of cholesterol biosynthesis after 24 h incubation, expressed as dpm/mg cell protein for CHO, ZR-78 and ZR-82 cells. Each value represents the average of three experiments, performed in duplicate, \pm SE. There is no significant difference between the ZR-78 and ZR-82 cells and control cells. Panel D, rate of dolichol biosynthesis, after 24 h incubation, expressed as dpm/mg cell protein for CHO, ZR-78 and ZR-82 cells. Each value represents the average of three experiments, \pm SE. There is no significant difference between the ZR-78 and ZR-82 cells and control cells. The total protein content per flask was between 320 and 480 μ g.

tase activity correlated with the protein level (7). This was also the case for the reductase activity levels in CHO cells and the 97 kDa ER protein. However, we could not make any correlation between the two cell lines. Therefore, the activity data cannot be interpreted based on a direct correlation of the density levels of the two proteins. In addition, the ER protein may not be as active when the 90 kDa protein levels are low; the two proteins may be co-regulated in some fashion or the ER protein may be phosphorylated and thereby exhibit decreased activity. Cell fractionation studies of CHO cells to determine the relative contribution from each organelle are also difficult to interpret, due to cross contamination of the ER protein in the peroxisomal fraction (7) and the inhibition of the peroxisomal form by most density gradient media (6). Future studies will address the relative contribution of activity of each isoenzyme when appropriate probes become available.

The observed decrease in total reductase activity would predict that the rate of both sterol and non-sterol biosynthesis would be reduced in the mutant cells when starting with [³H] acetate as a substrate. Indeed, starting with [³H] acetate as a substrate demonstrated that the rates of both cholesterol and dolichols biosynthesis were significantly decreased in the mutant cells as compared to control CHO cells (Fig. 5).

To address the question of whether the decrease in isoprenoid biosynthesis, when starting with acetate as substrate, was strictly due to the decrease in reductase activity or also as a result of a deficiency in the peroxisomal isoprenoid enzymes catalyzing the conversion of mevalonate to FPP, we analyzed the rates of cholesterol and dolichol biosynthesis starting with [³H]mevalonate. The rates of both cholesterol and dolichol biosynthesis were decreased in the mutant cells as compared to the control cells (Fig.

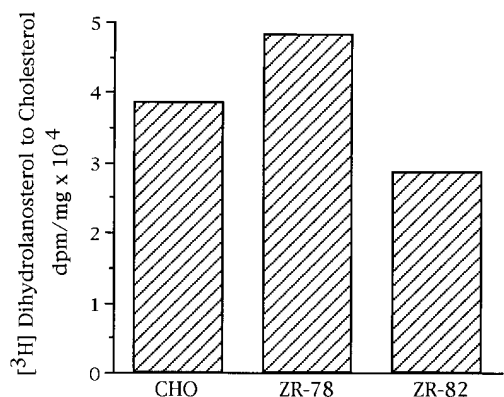


Fig. 8. Rate of biosynthesis of cholesterol in CHO and peroxisome-deficient ZR-78 and ZR-82 cells as measured by the incorporation of [³H]dihydrolanosterol. CHO and peroxisome-deficient ZR-78 and ZR-82 cells were first incubated for 6 h with 1 μ M lovastatin and then incubated for 24 h with [³H]dihydrolanosterol 6 μ Ci (1.0×10^6 dpm/nmol/flask) and cholesterol biosynthesis was determined as described in Materials and Methods. The rate of cholesterol biosynthesis is expressed as dpm/mg cell protein for CHO, ZR-78 and ZR-82 cells. Each value represents the average of two experiments. The total protein content per flask was between 240 and 400 μ g.

6). These data support the earlier observation that the enzymatic activities of mevalonate kinase, phosphomevalonate kinase, mevalonate diphosphate decarboxylase, isopentenyl diphosphate isomerase, and FPP synthase were significantly reduced in liver tissue obtained from patients with peroxisome-deficient diseases (12).

A number of studies support the conclusion that the conversion of mevalonate to FPP occurs predominantly in peroxisomes while the conversion of FPP to squalene occurs in the ER (1). However, recent studies suggest that peroxisomes like the ER may participate in the conversion of lanosterol to cholesterol as well as in some of the steps required for dolichols biosynthesis (1, 18, 31). Therefore, we incubated the cells with [³H]farnesol and [³H]dihydro-

lanosterol to determine whether peroxisomal-deficient cells have a defect in the conversion of FPP to cholesterol and dolichols and in the conversion of dihydrolanosterol to cholesterol. As shown in Fig. 7 there was no difference in the rate of dolichol biosynthesis when cells were incubated with farnesol. These results would suggest that peroxisomal enzymes are not required for dolichol biosynthesis. However, the rate of cholesterol biosynthesis was decreased in the peroxisomal-deficient cells after incubation with farnesol for 12 h but not when cells were incubated for 24 h (Fig. 7). These results suggest that one or more of the reactions involved in the conversion of FPP to cholesterol may occur in the peroxisomes. When the rate of lanosterol biosynthesis was measured, the peroxisomal-deficient cells exhibited 2- to 2.5-fold higher rates than those of the control cells, Fig. 9. These data are in agreement with previous reports demonstrating that pure peroxisomes in an in vitro system were able to synthesize cholesterol when incubated with dihydrolanosterol as a substrate, but not when incubated with squalene (1), and studies that reported the presence of dihydrolanosterol oxidase, steroid-14-reductase, steroid-3-ketoreductase, and steroid-8-isomerase activities in rat liver peroxisomes (18). It is significant to note, however, that even though the rate of accumulation of lanosterol was higher in the peroxisomal-deficient cell lines, the rate of cholesterol biosynthesis was similar to control cells when farnesol or dihydrolanosterol were used as substrates for 24 h. These results indicate that the deficiency of the enzyme or enzymes in the cells resulting in the accumulation of lanosterol is not the rate-limiting step for cholesterol biosynthesis from FPP or dihydrolanosterol, as after 24 h the cells display similar rates of cholesterol biosynthesis. Alternatively, during this time period, the ER cholesterol biosynthesis enzymes are up-regulated and may compensate for the peroxisomal deficiency.

Part of the discrepancy between our results and those of van Heusden et al. (26) may be due to the technique used for determining cholesterol biosynthesis. In their proce-

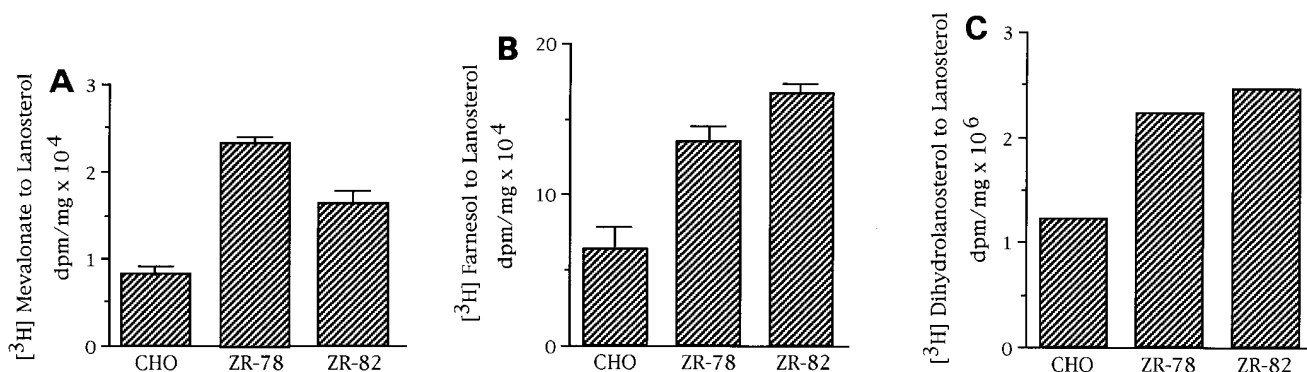


Fig. 9. Rate of biosynthesis of lanosterol in CHO and peroxisome-deficient ZR-78 and ZR-82 cells as measured by the incorporation of [³H]mevalonate, [³H]farnesol, and [³H]dihydrolanosterol. Cells were incubated with [³H] mevalonate, [³H] farnesol, for 24 h or [³H]dihydrolanosterol as indicated in legends of Figs. 6–8. The rate of lanosterol biosynthesis is expressed as dpm/mg cell protein for CHO, ZR-78 and ZR-82 cells. Each value represents the average of three experiments, performed in duplicate, \pm SE, ($P < 0.05$ for ZR-78 and ZR-82 cells vs. control cells), except for the conversion of dihydrolanosterol to lanosterol where the average of two experiments is given. Similar increases in lanosterol biosynthesis were observed after incubation with farnesol for 12 h (data not shown).

dure, as stated by the authors (26), ³H-labeled sterols very similar to [³H]-cholesterol were not resolved. As lanosterol is clearly accumulated in the mutant cells, it is probable that their values not only represent cholesterol but the sum of cholesterol and lanosterol, thus resulting in higher rates of total sterol biosynthesis. In addition, the reported HMG-CoA reductase activity of wild type CHO cells in their study (137 pmol/min/mg), is considerably lower than the activity measured in our study (240 pmol/min/mg) or that reported by several other groups (40–42).

In summary, we have shown that peroxisomal-deficient CHO cell lines have decreased rates of cholesterol biosynthesis when acetate, mevalonate, or farnesol are used as substrates. These data are in agreement with previous studies in peroxisomal-deficient human fibroblast cell lines which also demonstrated impaired rates of cholesterol biosynthesis (21, 22). This decrease is most likely due to the deficiency in the peroxisomal cholesterol biosynthesis enzymes in these cells. This conclusion is supported by the observation that while control CHO cells can grow indefinitely in media containing lipoprotein-deficient serum, in contrast, the peroxisomal-deficient CHO cells are able to survive for only 10 days (data not shown). In addition, we have demonstrated that in the mutant cells the 90 kDa peroxisomal HMG-CoA reductase protein is localized to the cytosol, that non-sterol biosynthesis is also decreased when acetate or mevalonate are used as substrates, but not when farnesol is used, and that the peroxisomal-deficient CHO cells accumulate lanosterol. ■

This work was supported by National Institutes of Health grant DK 32852, and in part by grants from The Council for Tobacco Research, USA.

Manuscript received 18 December 1997, in revised form 31 March 1998, and in re-revised form 4 May 1998.

REFERENCES

1. Krisans, S. K. 1996. Cell compartmentalization of cholesterol biosynthesis. *Ann. N.Y. Acad. Sci.* **804**: 142–164.
2. Thompson, S. L., and S. K. Krisans. 1990. Rat liver peroxisomes catalyze the initial steps in cholesterol synthesis. *J. Biol. Chem.* **265**: 5731–5735.
3. Hovik, R., B. Brodal, K. Bartlett, and H. Osmundsen. 1991. Metabolism of acetyl-CoA by isolated peroxisomal fractions: formation of acetate and acetoacetyl-CoA. *J. Lipid Res.* **32**: 993–999.
4. Krisans, S. K., N. Rusnak, G. A. Keller, and P. A. Edwards. 1988. Localization of 3-hydroxy-3-methylglutaryl coenzyme A synthase in rat liver peroxisomes. *J. Cell Biol.* **107**: 122.
5. Keller, G. A., M. C. Barton, D. J. Shapiro, and S. J. Singer. 1985. 3-Hydroxy-3-methylglutaryl-coenzyme A reductase is present in peroxisomes in normal rat liver cells. *Proc. Natl. Acad. Sci. USA.* **82**: 770–774.
6. Keller, G. A., M. Pazirandeh, and S. K. Krisans. 1986. 3-Hydroxy-3-methylglutaryl coenzyme A reductase localized in rat liver peroxisomes and microsomes of control and cholestyramine-treated animals: quantitative biochemical and immunoelectron microscopical analysis. *J. Cell Biol.* **103**: 875–886.
7. Engfelt, W. H., J. E. Shackelford, N. Aboushadi, N. Jessani, K. Masuda, V. G. Paton, G. A. Keller, and S. K. Krisans. 1997. The characterization of the UT-2 cells. The induction of peroxisomal 3-hydroxy-3-methylglutaryl coenzyme A. *J. Biol. Chem.* **272**: 24579–24587.

8. Stamellos, K. D., J. E. Shackelford, R. D. Tanaka, and S. K. Krisans. 1992. Mevalonate kinase is localized in rat liver peroxisomes. *J. Biol. Chem.* **267**: 5560–5568.
9. Biardi, L., A. Sreedhar, A. Zokei, N. B. Vartak, J. E. Shackelford, G. A. Keller, and S. K. Krisans. 1994. Mevalonate kinase is predominantly localized in peroxisomes and is defective in patients with peroxisome-deficient disorders. *J. Biol. Chem.* **269**: 1197–1205.
10. Biardi, L., and S. K. Krisans. 1996. Compartmentalization of cholesterol biosynthesis: conversion of mevalonate to farnesyl diphosphate occurs in the peroxisomes. *J. Biol. Chem.* **271**: 1784–1788.
11. Paton, V. G., J. E. Shackelford, and S. K. Krisans. 1997. Cloning and subcellular localization of hamster and rat isopentenyl diphosphate dimethylallyl diphosphate isomerase. A PTS1 motif targets the enzyme to peroxisomes. *J. Biol. Chem.* **272**: 18945–18950.
12. Krisans, S. K., J. Ericsson, P. A. Edwards, and G. A. Keller. 1994. Farnesyl-diphosphate synthase is localized in peroxisomes. *J. Biol. Chem.* **269**: 14165–14169.
13. Tanaka, R. D., L. Y. Lee, B. L. Schafer, V. J. Kratunis, W. A. Mohler, G. W. Robinson, and S. T. Mosley. 1990. Molecular cloning of mevalonate kinase and regulation of its mRNA levels in rat liver. *Proc. Natl. Acad. Sci. USA.* **87**: 2872–2876.
14. Chambliss, K. L., C. A. Slaughter, R. Schreiner, G. F. Hoffman, and M. Gibson. 1996. Molecular cloning and expression of human phosphomevalonate kinase and identification of consensus peroxisomal targeting sequence (PTS). *J. Biol. Chem.* **271**: 17330–17334.
15. Toth, J. M., and L. Huwyler. 1996. Molecular cloning and expression of cDNAs encoding human and yeast pyrophosphate decarboxylase. *J. Biol. Chem.* **271**: 7895–7898.
16. Xuan, J. M., J. Kowalski, A. F. Chambers, and D. T. Denhardt. 1994. A human promyelocyte mRNA transiently induced by TPA is homologous to yeast IPP isomerase. *Genomics.* **20**: 129–131.
17. Subramani, S. 1993. Protein import into peroxisomes and biogenesis of the organelle. *Annu. Rev. Cell Biol.* **9**: 445–478.
18. Appelkvist, E. L., M. Reinhart, R. Fischer, J. Billheimer, and G. Dallner. 1990. Presence of individual enzymes of cholesterol biosynthesis in rat liver peroxisomes. *Arch. Biochem. Biophys.* **282**: 318–325.
19. Lazarow, P. B., and H. W. Moser. 1995. Disorders of peroxisome biogenesis. *In* The Metabolism and Molecular Basis of Inherited Diseases. C. R. Scriver, A. L. Beaudet, W. S. Sly, and D. Valle, editors. McGraw-Hill, Inc., New York. 2287–2324.
20. Van den Bosch, H., R. B. H. Schutgens, R. J. A. Wanders, and J. M. Tager. 1992. Biochemistry of peroxisomes. *Annu. Rev. Biochem.* **61**: 157–197.
21. Hodge, V. J., S. J. Gould, S. Subramani, H. W. Moser, and S. K. Krisans. 1991. Normal cholesterol synthesis in human cells requires functional peroxisomes. *Biochem. Biophys. Res. Commun.* **181**: 537–541.
22. Mandel, H., M. Getsis, M. Rosenblat, M. Bernat, and M. Avriam. 1995. Reduced cellular cholesterol content in peroxisome-deficient fibroblasts is associated with impaired uptake of the patient's low density lipoprotein and with reduced cholesterol synthesis. *J. Lipid Res.* **36**: 1385–1391.
23. Zoeller, R. A., and C. R. Raetz. 1986. Isolation of animal cell mutants deficient in plasmalogen biosynthesis and peroxisome assembly. *Proc. Natl. Acad. Sci. USA.* **83**: 5170–5174.
24. Morand, O. H., R. A. Zoeller, and C. R. Raetz. 1988. Disappearance of plasmalogens from membranes of animal cells subjected to photosensitized oxidation. *J. Biol. Chem.* **263**: 11597–11606.
25. Zoeller, R. A., L. A. Allen, M. J. Santos, P. B. Lazarow, T. Hashimoto, A. M. Tartakoff, and C. R. Raetz. 1989. Chinese hamster ovary cell mutants defective in peroxisomes assembly. Comparison to Zellweger syndrome. *J. Biol. Chem.* **264**: 14165–14169.
26. Van Heusden, G. P. H., J. R. C. M. van Beckhoven, R. Thieringer, C. R. H. Raetz, and W. A. Wirtz. 1992. Increased cholesterol synthesis in Chinese hamster ovary cells deficient in peroxisomes. *Biochim. Biophys. Acta.* **1126**: 81–87.
27. Plutner, H., H. W. Davidson, J. Sarasate, and W. E. Balch. 1992. Morphological analysis of protein transport from the ER to Golgi membrane in digitonin-permeabilized cells: role of the P58 containing compartment. *J. Cell Biol.* **119**: 1197–1205.
28. Tanaka, R. D., P. A. Edwards, S. F. Lan, and A. M. Fogelman. 1983. Regulation of 3-hydroxy-3-methylglutaryl coenzyme A reductase activity in avian myoblasts. Mode of action of 25-hydroxycholesterol. *J. Biol. Chem.* **258**: 13331–13339.
29. Keller, R. K., S. T. Nellis, and L. Cuadrado-Simonet. 1989. A rapid

- procedure for the separation and analysis of metabolites of the sterol and dolichol pathways. *Chem. Phys. Lipids*. **51**: 261–267.
30. Goldstein, J. L., and M. S. Brown. 1990. Regulation of the mevalonate pathway. *Nature*. **343**: 425–430.
 31. Grunler, J., J. M. Olsson, and G. Dallner. 1995. Estimation of dolichol and cholesterol synthesis in microsomes and peroxisomes isolated from rat liver. *FEBS Lett.* **358**: 230–232.
 32. Stamellos, K. D., J. E. Shackelford, I. Shechter, G. Jiang, D. Conrad, G. A. Keller, and S. K. Krisans. 1993. Subcellular localization of squalene synthase in rat hepatic cells: biochemical and immunohistochemical evidence. *J. Biol. Chem.* **268**: 12825–12836.
 33. Crick, D. C., D. A. Andreas, and C. J. Waechter. 1995. Farnesol is utilized for protein isoprenylation and the biosynthesis of cholesterol in mammalian cells. *Biochem. Biophys. Res. Commun.* **211**: 590–599.
 34. Thieringer, R., and C. R. H. Raetz. 1993. Peroxisome-deficient Chinese hamster ovary cells with point mutations in peroxisome assembly factor-1. *J. Biol. Chem.* **268**: 12631–12636.
 35. Allen, L. A. H., and C. R. H. Raetz. 1992. Partial phenotypic suppression of a peroxisome-deficient animal cell mutant treated with aminoglycoside G418. *J. Biol. Chem.* **267**: 13191–13199.
 36. Shimozawa, N., T. Tsukamoto, Y. Suzuki, T. Orii, Y. Shirayoshi, T. Mori, and Y. Fujiki. 1992. A human gene responsible for Zellweger syndrome that affects peroxisome assembly. *Science*. **350**: 1132–1134.
 37. Faust, P. L., and M. E. Hatten. 1997. Targeted deletion of the PEX2 peroxisome assembly gene in mice provides a model for Zellweger syndrome, a human neuronal migration disorder. *J. Cell Biol.* **139**: 1293–1305.
 38. Santos, M. J., T. Imanaka, H. Shio, G. M. Small, and P. B. Lazarow. 1988. Peroxisomal membrane ghosts in Zellweger syndrome-aberrant organelle assembly. *J. Biol. Chem.* **263**: 10502–10509.
 39. Schram, A. W., A. Stijland, T. Hashimoto, R. J. A. Wanders, H. van den Bosch, and J. M. Tager. 1986. Biosynthesis and maturation of peroxisomal beta-oxidation enzymes in fibroblasts in relation to the Zellweger syndrome and infantile Refsum disease. *Proc. Natl. Acad. Sci. USA.* **83**: 6156–6158.
 40. Mosley, S. T., M. S. Brown, R. G. W. Anderson, and J. L. Goldstein. 1983. Mutant clone of Chinese hamster ovary cells lacking 3-hydroxy-3-methylglutaryl coenzyme A reductase. *J. Biol. Chem.* **258**: 13875–13881.
 41. Nakanishi, M., J. L. Goldstein, and M. S. Brown. 1988. Multivalent control of 3-hydroxy-3-methylglutaryl coenzyme A reductase. *J. Biol. Chem.* **263**: 8929–8937.
 42. Straka, M. S., and S. R. Panini. 1995. Post-translational regulation of 3-hydroxy-3-methylglutaryl coenzyme A reductase by mevalonate. *Arch. Biochem. Biophys.* **317**: 235–243.